New Limits on Doubly Charged Bileptons from LEP Data, and Search at Future Electron–Positron and Electron–Photon Colliders

E. M. Gregores[1,2], A. Gusso[1,3] and S. F. Novaes[1]

[1] *Instituto de Física Teórica, Universidade Estadual Paulista, 01405–900 São Paulo – SP, Brazil*

[2] *Department of Physics, University of Wisconsin Madison, WI 53706, USA*

[3] *Instituto de Física Corpuscular - C.S.I.C., Universitat de València, E-46071 València, Spain*

Abstract

We show that the accumulated LEP-II data taken at $\sqrt{s} = 130$ to 206 GeV can establish more restrictive bounds on doubly charged bilepton couplings and masses than any other experiment so far. We also analyze the discovery potential of a prospective linear collider operating in both e^+e^- and $e\gamma$ modes.

14.80.-j, 12.60.-i, 13.88.+e

I. INTRODUCTION

Bileptons are bosons carrying double leptonic number that are predicted by some extensions of the Standard Model like $SU(15)$ based GUT theory [1], 3-3-1 model [2], and left–right symmetric models [3]. They can either be scalar or vector particles with different charges, *i.e.* neutral, singly, or doubly charged. In the 3-3-1 model, the symmetry breaking $SU(3)_L \times U(1)_X \to SU(2)_L \times U(1)$ is responsible for the appearance of vector bileptons, while in the left-right model, based on $SU(2)_L \times SU(2)_R \times U(1)_{B-L}$, the bileptons correspond to the doubly charged scalar bosons present in the symmetry breaking sector.

Bileptons can participate in a large variety of processes, both at low and high energies. However, no signal has yet been found, and bounds on their masses and couplings could be obtained from the analysis of lepton number violating processes [4], and muonium–antimuoniuon (M–$\overline{M}$) conversion [5,6] experiments. The existing mass limits for both singly and doubly charged bosons [5,7] are all model dependent. These bounds still allow the existence of low–mass bileptons with a small coupling constant. The limits from high energy experiments [6] like e^+e^- collisions are, in principle, less restrictive than the low energy bounds.

In this paper we explore the production of doubly charged bileptons in both e^+e^- and $e\gamma$ colliders, looking for the most promising signature for identifying these particles: an isolated same sign, planar, and p_T balanced two muons(antimuons) event [6,8,9]. We made a model independent analysis, working in the context of a general effective $SU(2)_L \times U(1)_Y$ Lagrangian that couples bileptons to leptons [6]

$$\mathcal{L} = \lambda_1 \bar{\ell}^c i\sigma_2 \ell L_1 + \tilde{\lambda}_1 \overline{e}^c e \tilde{L}_1 + \lambda_2 \overline{\ell}^c \gamma^\mu e L_{2\mu} + \lambda_3 \overline{\ell}^c i\sigma_2 \vec{\sigma} \ell \cdot \vec{L}_3 + \text{h.c.} \,, \tag{1}$$

where $\ell = (e_L, \nu_L)$ are left–handed $SU(2)_L$ lepton doublets, and $e = e_R$ are right–handed charged singlet leptons. The charge conjugated fields are defined as $\overline{\ell}^c = (\ell^c)^\dagger \gamma^0 = -\ell^T C^{-1}$. The subscript of the bilepton fields $L = 1, 2, 3$ indicates whether they are singlet, doublet, or triplet under $SU(2)_L$. The terms concerning the doubly charged bileptons can be written as

$$\mathcal{L}^{--} = \tilde{\lambda}_1^{ij}\, \overline{e}_i^c P_R\, e_j \tilde{L}_1^{--} + \lambda_2^{ij}\, \overline{e}_i^c \gamma^\mu P_R\, e_j L_{2\mu}^{--} + \sqrt{2}\, \lambda_3^{ij}\, \overline{e}_i^c P_L\, e_j L_3^{--} + \text{h.c.} \,, \tag{2}$$

where e_i represent the charged leptons with flavor indices $i, j = 1, 2, 3$, and $P_{R(L)} = (1 \pm \gamma_5)/2$ are the helicity projectors. We will consider here only flavor diagonal bilepton couplings since very restrictive bounds are imposed by low–energy experiments when flavor violation can take place [4,6]. These couplings will also be considered real to avoid CP violating processes.

II. LIMITS FROM LEP

The whole LEP program has been very successful. They were able to achieve both energy and luminosity beyond the values initially expected. However no evidence for new physics has yet been found. From the non observation of pair produced bileptons model independent lower limits on the masses of these particles can be established to be close to 100 GeV. However, the present most stringent bounds on the mass and coupling of doubly charged bileptons come from the results of muonium–antimuonium conversion experiments

[5]. For flavor diagonal couplings, these measurements require that the ratio of the bilepton coupling and its mass must satisfy $\tilde{\lambda}_1/M_B < 0.20$ TeV^{-1} (90% C.L.), $\lambda_2/M_B < 0.27$ TeV^{-1} (95% C.L.), and $\lambda_3/M_B < 0.14$ TeV^{-1} (90% C.L.).

We found that these limits can be overridden for the mass range kinematically accessible at LEP collider. The occurrence of a high–energy event presenting just a p_T balanced co–planar pair of same–sign leptons, notably muons or antimuons, would be a striking evidence for the presence of a bilepton. Since there is no Standard Model background for this kind of process, the observation of one of such dimuon event would already constitute a important step towards the bilepton discovery. From the non observation of such event a 90 (95)% C.L. upper bound on the values of λ and M_B can be obtained based on the predited number of 2.3 (3.0) events.

This signature results predominantly from the process depicted in Fig. 1(a), and its cross-section has been evaluated in the equivalent particle approximation [10]. The deviation from the exact calculation is expected to be small since this process is dominated by events where the incident particle is scattered at a very small angle. The relevant cross-section is given by,

$$\sigma(E_{e^+},\hat{s})_{e^+e^-\to\mu^-\mu^-} = \int_{x_{\min}}^{1} dx\, F_{e^+}^{e^-}(x,E_{e^+})\,\sigma(\hat{s})_{e^-e^-\to\mu^-\mu^-}, \tag{3}$$

where $F_{e^+}^{e^-}(x,E_{e^+})$ is the equivalent electron distribution function of the initial positron. It gives the probability that an electron with energy $E_{e^-} = xE_{e^+}$ is emitted from a positron beam with energy E_{e^+}. The same holds true for the positron contents of the electron. This distribution is [11]

$$F_{e^+}^{e^-}(x,E_{e^+}) = \frac{1}{2}\left\{\frac{\alpha}{2\pi}\left[\ln\left(\frac{E_{e^+}}{m_e}\right)^2 - 1\right]\right\}^2 \left(\frac{1}{x}\right)\left(\frac{4}{3} + x - x^2 - \frac{4}{3}x^3 + 2x(1+x)\ln x\right). \tag{4}$$

The cross-section for the subprocess $e^-e^- \to \mu^-\mu^-$ is

$$\sigma(\hat{s}) = S\frac{\lambda^4\hat{s}}{24\pi[(\hat{s}-M_B^2)^2 + M_B^2\Gamma^2]}\ , \tag{5}$$

where $\Gamma = G\lambda^2 M_B/(8\pi)$ is the s-channel resonance width for a bileptons of mass M_B, $\hat{s} = xs$ is the subprocess squared center of mass energy, $S = 3,\ 1,\ 12$ and $G = 3,\ 1,\ 6$ for $\tilde{L}_1^{--}$, $L_{2\mu}^{--}$ and L_3^{--}, respectively.

We present in Tab. I the integrated luminosities for the different LEP energies we used in our calculations [12]. The total number of expected events (pairs of muons or antimuons with total invariant mass M_B) is calculated considering the luminosities obtained at center of mass energies that are larger than the bilepton mass, *i.e.*,

$$N(M_B) = 2\sum_i \Theta(\sqrt{s_i} - M_B)\,\mathcal{L}(\sqrt{s_i})\int_{\hat{s}=4m_\mu^2}^{s_i} d\hat{s}\ \sigma(\sqrt{s_i}/2,\hat{s})_{e^+e^-\to\mu^-\mu^-} \tag{6}$$

where $N(M_B)$ is the number of expect events with mass M_B, $\mathcal{L}(\sqrt{s_i})$ assumes the values in Tab. I. The factor 2 stands for the fact that $\sigma_{e^+e^-\to\mu^-\mu^-} = \sigma_{e^+e^-\to\mu^+\mu^+}$.

In Fig. 2(a) and (b) we present, respectively, the limits on $L_{2\mu}^{--}$ and L_3^{--} coupling constant that are imposed by the LEP data as a function of the bilepton mass. The solid line

corresponds to 2.7 fb^{-1} of integrated luminosity collected at energies ranging from 130 GeV up to 206 GeV, by the four LEP collaborations. We also show the exclusion areas in the λ–M_B parameter space imposed by M–$\overline{M}$ conversion experiments. The limits from the LEP data on $\tilde{\lambda}_1$, and the region already excluded by M–$\overline{M}$ conversion, corresponding to $\tilde{\lambda}_1/M_B < 0.20$ TeV^{-1} are not shown in Fig. 2 but can be readily obtained from the limits for λ_3 using the fact that $\tilde{\lambda_1} = \sqrt{2}\lambda_3$. In order to obtain these results we have taken into account an efficiency of 90% for dimuon reconstruction and a geometric acceptance of $|\cos\theta| < 0.9$. This was a conservative choice for the geometric acceptance since we assumed the L3 value and all other experiments have larger acceptances. The maximum allowed values of λ/M_B at LEP are smaller than those obtained from muonium–antimuonium conversion by a factor of two for most of the bilepton mass range.

III. SEARCH AT FUTURE LINEAR COLLIDERS

A. Electron-Positron Collider

Amid the efforts that are under way to determine the potentiality of proposed linear colliders to discover new physics [13], studies on bilepton searches have been carried out mostly for its e^-e^- collider operation mode [6,9,14]. We concentrate here on the potential of the e^+e^- and $e\gamma$ operation modes to discover doubly charged bileptons. We have assumed some representative values for the energy and luminosity of new electron–positron machine [15], namely $\sqrt{s} = 500$, 800, and 1000 GeV with $\mathcal{L} = 500$ fb^{-1}. This integrated luminosity is expected to be achieved in one or two years of the collider operation.

We evaluated the e^+e^- operation mode in a similar way we did for LEP. In Fig. 3, we plot the 95% confidence level discovery region in the λ–M_B parameter space. In this figure, we also plotted the region of the parameter space already excluded by muonium–antimuonium conversion experiments. We considered a 90% dimuon reconstruction efficiency. We did not consider a particular value for the geometric acceptance, since we estimated that a 5° aperture in the beam pipe region would not lead to more than 2% event loss.

If bileptons are indeed observed, and profusely produced, it will be possible to determine their mass, and to learn whether they are vector or scalar particles. In Fig. 4, we present the expected dimuon invariant mass differential cross section, for some specific values of the vector bilepton coupling, which shows the resonant peak on the bilepton mass. We have chosen for λ_2 the maximum value allowed by the present M–$\overline{M}$ limits, *i.e.*, $\lambda_2 = 0.27\ M_B$.

The discrimination between vector and scalar can be done based on the fact that the cross section for the process $e^-e^- \to \mu^-\mu^-$ changes with the polarization of the initial electron beams according to which of the three kind of bileptons participates in the reaction. The discrimination can also be done using the fact that a vector bilepton leads to an angular distribution of the final state muons that is different from the angular distribution that would be observed if bileptons were scalars. The dependences on the initial beam polarizations (P_1 and P_2) are shown in Tab. II, as well as the dependence on the angular distribution of the produced muons.

A discrimination based on the initial beam polarization is very promising since in the next generation of linear colliders one expects up to 80% of polarization for the electron beam. Assuming that the electron emitted from the positron beam is kept unpolarized

($P_2 = 0$), we can see that, as the polarization of the electron beam (P_1) increases, the cross section for the process mediated by $\tilde{L}_1^{--}$ increases while the cross section for the process mediated by L_3^{--} decreases. On the other hand, the insensitivity to P_1 would indicate the presence of a vector bilepton, as can be seen from Tab. II. However, if $\tilde{L}_1^{--}$ and L_3^{--} get mixed, the dependence on P_1 can be too small ($\tilde{\lambda}_1 = \sqrt{2}\lambda_3$) to be observed, and it would not be possible to distinguish between vectors and scalars by looking at the electron beam polarization dependence of the cross-section.

The alternative would be to examine the angular distribution of the final state muons. In Fig. 5 we can see the difference between the angular distribution of reactions mediated by scalar and vectorial bileptons at $\sqrt{s} = 500$ GeV. However, when the bilepton mass is relatively small, like for a 150 GeV bilepton depicted in Fig. 5, the angular distributions for vector and scalar bileptons are quite similar. In this case, to distinguish vector from scalar particle it will require the knowledge of the bilepton mass with good accuracy. Fortunately, as can be seen from Fig. 5, the smaller the bilepton mass the bigger is the production cross-section. This may help to make the identification task easier since more events are expected in this case for a given value of the coupling constant.

B. Electron-Photon Collider

Projects for future linear colliders include the possibility to transform the initial e^+e^- machine into an $e\gamma$ or $\gamma\gamma$ collider with comparable energy and luminosity [16]. In these machines, a highly energetic photon beam is generated by Compton backscattering low energy photons emitted by a laser. The high energy backscattered photons are then made to collide with the opposite incoming beam. For a non–polarized collider, the backscattered photon distribution function is given by [17],

$$f_e^\gamma(x) = \frac{2}{\sigma^0}\left[\frac{1}{1-x} + 1 - x - 4r(1-r)\right], \tag{7}$$

where x is the fraction of the electron momentum carried by the photon, $r = x/[y(1-x)]$, and

$$\sigma^0 = \left(2 - \frac{8}{y} - \frac{16}{y^2}\right)\ln(y+1) + 1 + \frac{16}{y} - \frac{1}{(y+1)^2}\ , \tag{8}$$

where $y \approx 15.3\, E_B\, \omega_0$, with the parent electron energy E_B expressed in TeV, and the laser energy ω_0 in eV. A maximum value $y = 4.8$ is usually adopted to avoid electron regeneration through pair production. This is the y value we used in our analysis.

In the $e\gamma$ collider, bileptons would be produced as a s-channel resonance through the diagram depicted in Fig. 1(b). Similarly to the treatment we employed for e^+e^- colliders, we also assumed here that the positron escapes unobserved down the beam pipe. The cross-section for the process $e^-\gamma \to \mu^-\mu^-$ in the equivalent particle approximation is given by,

$$\sigma_{e^-\gamma\to\mu^-\mu^-} = \int_{x_1^{\min}}^{x_1^{\max}} \int_{x_2^{\min}}^{1} dx_1\, dx_2\, f_e^\gamma(x_1)\, F_\gamma^e(x_2)\, \hat{\sigma}_{e^-e^-\to\mu^-\mu^-} \tag{9}$$

where $f_e^\gamma(x_1)$ is given by Eq. (7), and $F_\gamma^e(x_2)$ is the distribution function of the equivalent electron carrying a fraction x_2 of the photon energy,

$$F_\gamma^e(x_2) = \frac{\alpha}{\pi}\left[x_2^2 + (1-x_2)^2\right]\ln\frac{E_\gamma}{m_e}\,. \tag{10}$$

We also determined the potential of the $e\gamma$ collider to discover bileptons considering the observation of a single event. It has been assumed that the luminosity of the $e\gamma$ mode will be comparable to its parent e^+e^- mode. In Fig. 6 we plot the 95% confidence level discovery region in the λ–M_B parameter space. In this figure, we also plotted the region of the parameter space already excluded by muonium–antimuonium conversion experiments. We can see that an $e\gamma$ collider is more efficient for the search of bileptons than the e^+e^- collider. This is expected since the laser backscattering mechanism (Fig. 1(b)) is capable to generate a large amount of hard photons when compared with the usual bremsstrahlung subprocess (Fig. 1(a)).

If the bileptons are discovered and a fairly large amount of events is collected, we can use the same procedure, based on the electron polarization and angular distribution of final state muons, to determine their mass and spin. In Fig. 7, we present the expected event distribution as a function of the muon (or antimuon) pair invariant mass. As in Fig. 4 the value of λ is the maximum allowed by the present M–$\overline{M}$ limits, *i.e.*, $\lambda_2 = 0.27\ M_B$. The angular distribution follows the same pattern as the one presented in Fig. 5.

IV. DISCUSSIONS AND CONCLUSIONS

In this article we have shown that new and more stringent limits on the coupling constants and masses of doubly charged bileptons can be obtained from LEP-II data. As for the limits from M–$\overline{M}$ conversion, our results apply to the case of flavor–diagonal bilepton couplings. These stringent bounds result from the fact that the integrated luminosity collected by the LEP Collaborations at energies above 189 GeV is very large. In order to obtain the new limits on λ and M_B we have applied the equivalent particle approximation method. It is expected that an exact tree level calculation of the cross-section would lead to only minor corrections to our results [10]. A few percent uncertainty in the cross-sections translates into even smaller corrections to the curves in Figs. 2, 3 and 6 because the cross-sections are proportional to λ^2. Our results suggest that an accurate analysis taking into account detailed LEP detectors and data sample properties will be able to establish bounds on bilepton couplings and masses that overcome the present ones.

We have also shown that the construction of high energy linear accelerators could lead to a large increase in the sensitivity to the doubly charged bileptons. If these new particles are in the reach of these machines, a quite evident resonance peak should be observed without the need to scan the collision energy. The sensitivity to bileptons of the general purpose $e\gamma$ collider is of the same order of magnitude as the e^-e^- operating mode. In order to compare both operation modes we updated the results presented at Ref. [8] on bilepton search in e^-e^- colliders, to the luminosity of 500 fb^{-1} considered here. The reanalysis is straightforward and is based on the fact that the cross-section for the process $e^-e^- \to \mu^-\mu^-$ is proportional to the square of the bilepton coupling and the limits on λ will be proportional to $\sqrt{1/\mathcal{L}}$, where $\mathcal{L}$ is the collider luminosity. In Tab. III we compare the limits on λ_2 for the two kind

of colliders operating at $\sqrt{s} = 0.5$ and 1 TeV, with $\mathcal{L} = 500$ fb^{-1}. As it would be expected, the e^-e^- mode is, in general, more sensible than the $e\gamma$ mode. This advantage may be however illusory. The instantaneous luminosity delivered by the e^-e^- collider is expected to be half that of the e^+e^- with same beam characteristics because of the anti-pinch effect. This fact slightly diminishes the advantage of the e^-e^- mode over the $e\gamma$ mode for bilepton production. By comparing Fig. 3 with the values in Tab. III, we can see that the direct e^+e^- mode is clearly less sensitive than the other two operation modes. Nevertheless, it is much more sensitive than the present experiments.

In conclusion, a collider operating at e^+e^- or $e\gamma$ modes is quite sensitive to the resonant production of doubly charged bileptons. If bileptons are indeed observed in these machines we will probably be able to get a lot of information about then. Later, their properties could be thoroughly studied using the e^-e^- mode operating at $\sqrt{s} = M_B$.

ACKNOWLEDGMENTS

E.M.G. is grateful to University of Wisconsin for its kind hospitality. A.G. would like to thanks the hospitality at the Instituto de Fisica Corpuscular (IFIC-UV) were part of this work was carried on. S.F.N. is grateful to Fermilab for its hospitality. This work was supported by Conselho Nacional de Desenvolvimento Científico e Tecnológico (CNPq), by Fundação de Amparo à Pesquisa do Estado de São Paulo (FAPESP), by Programa de Apoio a Núcleos de Excelência (PRONEX), and by Fundação para o Desenvolvimento da UNESP (FUNDUNESP). A.G. was partially supported by Fundação Coordenação de Aperfeiçoamento de Pessoal de Nível Superior (CAPES).

REFERENCES

[1] P. H. Frampton and B.-H. Lee, Phys. Rev. Lett. **64**, 619 (1990).

[2] F. Pisano and V. Pleitez, Phys. Rev. D **46**, 410 (1992);
P. H. Frampton, Phys. Rev. Lett. **69**, 2889 (1992).

[3] J. C. Pati and A. Salam, Phys. Rev. D **10**, 275 (1974);
R. N. Mohapatra and J. C. Pati, Phys. Rev. D **11**, 566 (1975).

[4] P. Frampton and D. Ng, Phys. Rev. D **45**, 4240 (1992);
H. Fujii, S. Nakamura and K. Sasaki, Phys. Lett. B **299**, 342 (1993);
G. K. Leontaris, K. Tamvakis and J. D. Vergados, Phys. Lett. B **162**, 153 (1985);
U. Bellgardt *et al.*, Nucl. Phys. B **299**, 1 (1988);
J. D. Bjorken and S. Weinberg, Phys. Rev. Lett. **38**, 622 (1977).

[5] L. Willmann *et al.*, Phys. Rev. Lett. **82**, 49 (1999);
H. Fujii, Y. Mimura, K. Sasaki and T. Sasaki, Phys. Rev. D **49**, 559 (1994);
D. Chang, W.-Y. Keung, Phys. Rev. Lett. **62**, 2583 (1989).

[6] F. Cuypers and S. Davidson, Eur. Phys. J. C **2**, 503 (1998);
N. Leporé, B. Thorndyke, H. Nadeau and D. London, Phys. Rev. D **50**, 2031 (1994).

[7] M. B. Tully and G. C. Joshi, Phys. Lett. B **466**, 333 (1993);
P. H. Frampton and M. Harada, Phys. Rev. D **58**, 095013 (1998).

[8] F. Cuypers and M. Raidal, Nucl. Phys. B **501**, 3 (1997).

[9] P. H. Frampton and A. Rasin, Phys. Lett. B **482**, 129 (2000).

[10] V. N. Baier, V. S. Vadin and V. A. Khoze, Nucl. Phys. B **65**, 381 (1973);
M-S. Chen and P. Zerwas, Phys. Rev. D **12**, 187 (1975);
A. Zembrzuski and M. Krawczyk, *DESY HERA Workshop*, 617 (1991);
I. F. Ginzburg and V. G. Serbo, Phys. Rev. D **49**, 2623 (1994).

[11] T. Sjöstrand, Comp. Phys. Comm. **82**, 74 (1994).

[12] P. Abreu *et al.* (DELPHI Collaboration), Phys. Lett. B **485**, 45 (2000);
P. Bock *et al.* (LEP working group for Higgs boson searches), CERN-EP-2000-055 to appear in *35th Rencontres de Moriond on Electroweak Interactions and Unified Theories*, Les Arcs, France, 11 – 18 Mar 2000 ;
M. A. Bizouard *et al.* (LEP Working Group on Four Jets), CERN-OPEN-98-008;
M. Acciarri *et al.* (L3 Collaboration), Phys. Lett. B **485**, 85 (2000);
G. Abbiendi *et al.* (OPAL Collaboration), Phys. Lett. B **476**, 256 (2000);
R. Barate *et al.* (ALEPH Collaboration), Phys. Lett. B **469**, 287 (1999).

[13] See for instance M. Peskin, SLAC-PUB-8288, hep-ph/9910521.

[14] M. Raidal, Phys. Rev. D **57**, 2013 (1998).

[15] J. Bagger *et al.* (American Linear Collider Working Group), hep-ex/0007022. See also information available at `http://www.desy.de/s̃chreibr/physics-wg.html` and `http://www.slac.stanford.edu/xorg/ilc-trc/ilc-trchom.html`.

[16] V. I. Telnov, in *Proceedings of 4th International Workshop on Linear Colliders (1999)*, hep-ph/9910010;
I. F. Ginzburg, Nucl. Phys. Proc. Suppl. **82**, 367 (2000).

[17] D. L. Borden, D. A. Bauer and D. O. Caldwell, SLAC-PUB-5715, 1992 (*unpublished*);
idem Report No. UCSB-HEP-92-01, 1992 (*unpublished*);
idem Phys. Rev. D **48**, 4018 (1993).

TABLES

$\sqrt{s}$ (GeV)	133	161	172	183	189	192	196	200	202	206
$\mathcal{L}(\sqrt{s})$ (pb^{-1})	22	42	41	217	678	113	313	328	155	800

TABLE I. LEP integrated luminosities at different energies. The luminosity at $\sqrt{s} = 133$ GeV is the weighted average of the luminosities obtained at 130 GeV and 136 GeV.

	Polarization dependence	Angular dependence
$\tilde{L}_1^{--}$	$(1+P_1)(1+P_2)$	none
$L_{2\mu}^{--}$	$1-P_1P_2$	$1+\cos^2\theta^*$
L_3^{--}	$(1-P_1)(1-P_2)$	none

TABLE II. Angular and polarization dependence for $e^+e^- \to \mu^-\mu^-$ (θ^* is the C.M. angle).

M_B	$\lambda_2 \times 10^4$ (500 GeV)		$\lambda_2 \times 10^4$ (1 TeV)	
	e^-e^-	$e\gamma$	e^-e^-	$e\gamma$
200	2.50	2.40	1.46	4.72
300	0.96	3.22	1.36	5.55
400	0.60	4.21	1.23	6.64
500	0.11	—	1.10	7.73

TABLE III. Values of λ_2 that lead to the expected number of three events in the case $\mathcal{L} = 500$ fb^{-1}.

FIGURES

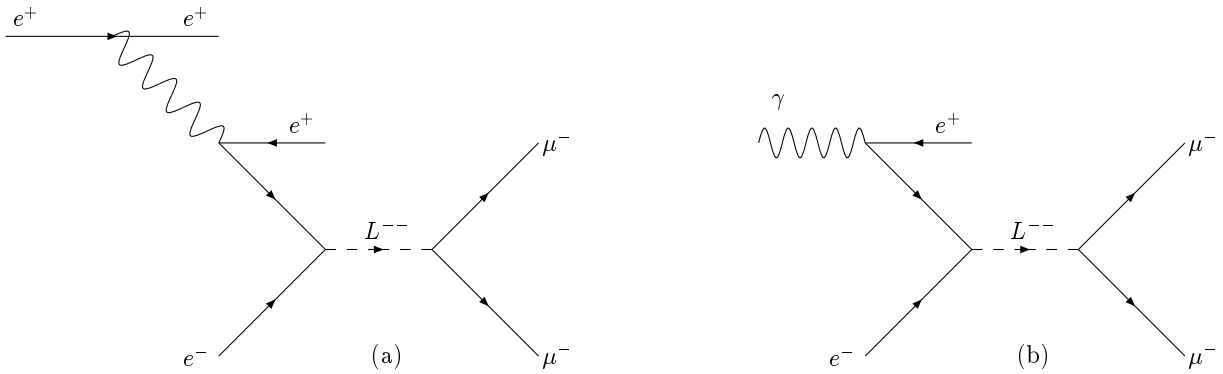

FIG. 1. Main contribution to the processes (a) $e^+e^- \to \mu^\pm\mu^\pm$ and (b) $e^-\gamma \to \mu^-\mu^-$.

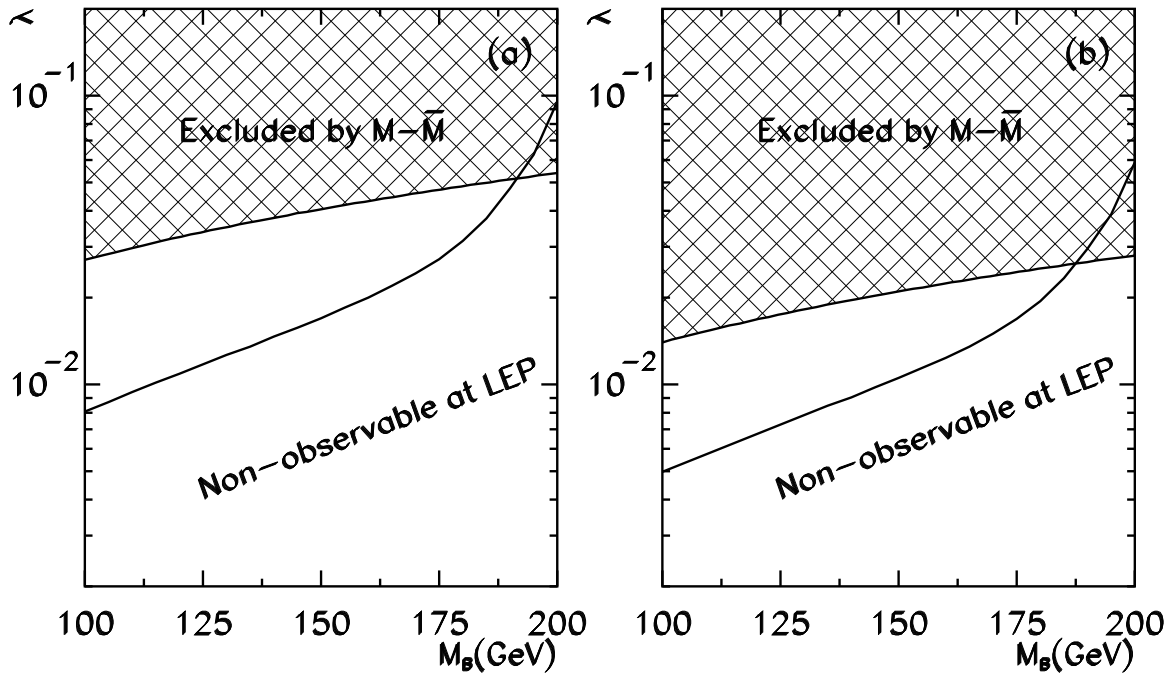

FIG. 2. Bilepton exclusion plot in the (M_B, λ) plane for LEP data. (a) limits on λ_2 (95% C.L.). (b) limits on λ_3 (90% C.L.). See comments on Sec. II for the limits on $\tilde{\lambda}_1$.

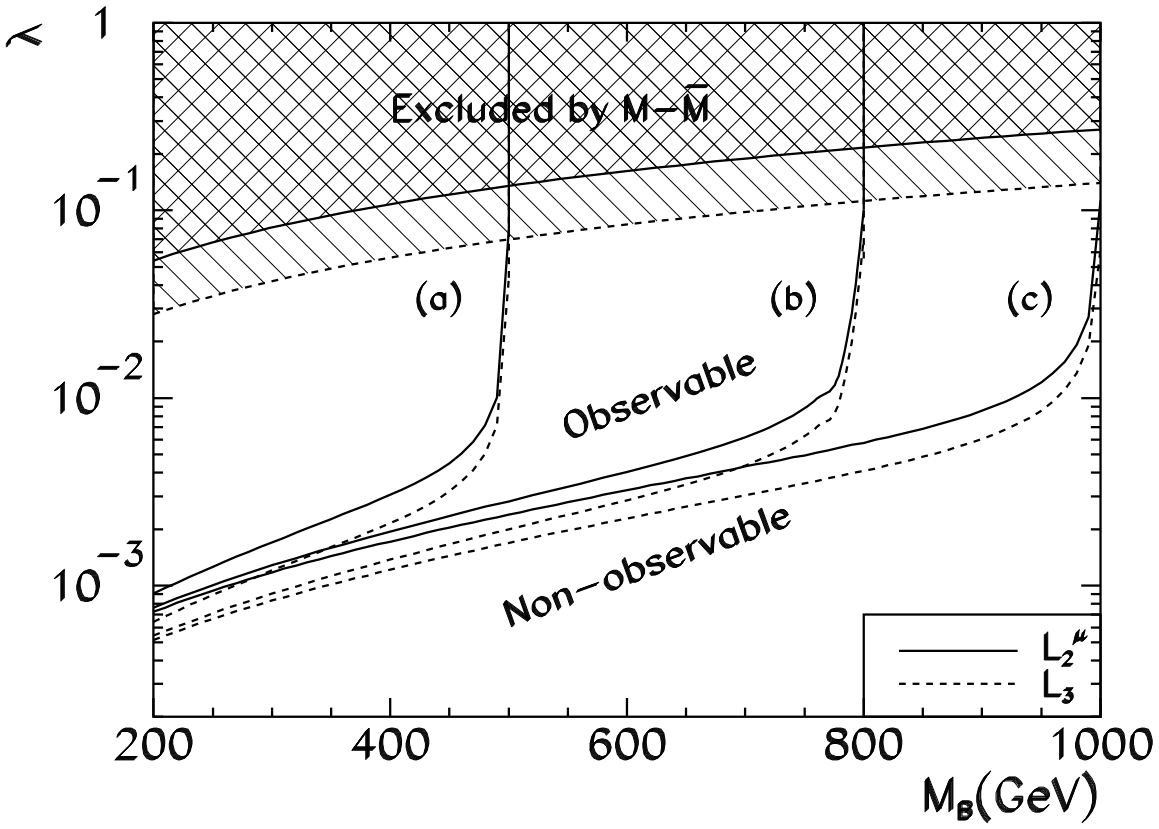

FIG. 3. Discovery region in the (M_B, λ) plane at 95% C.L., assuming $\mathcal{L} = 500\ fb^{-1}$ and $\sqrt{s} = 500$ (a), 800 (b), and 1000 (c) GeV, for a future e^+e^- linear collider.

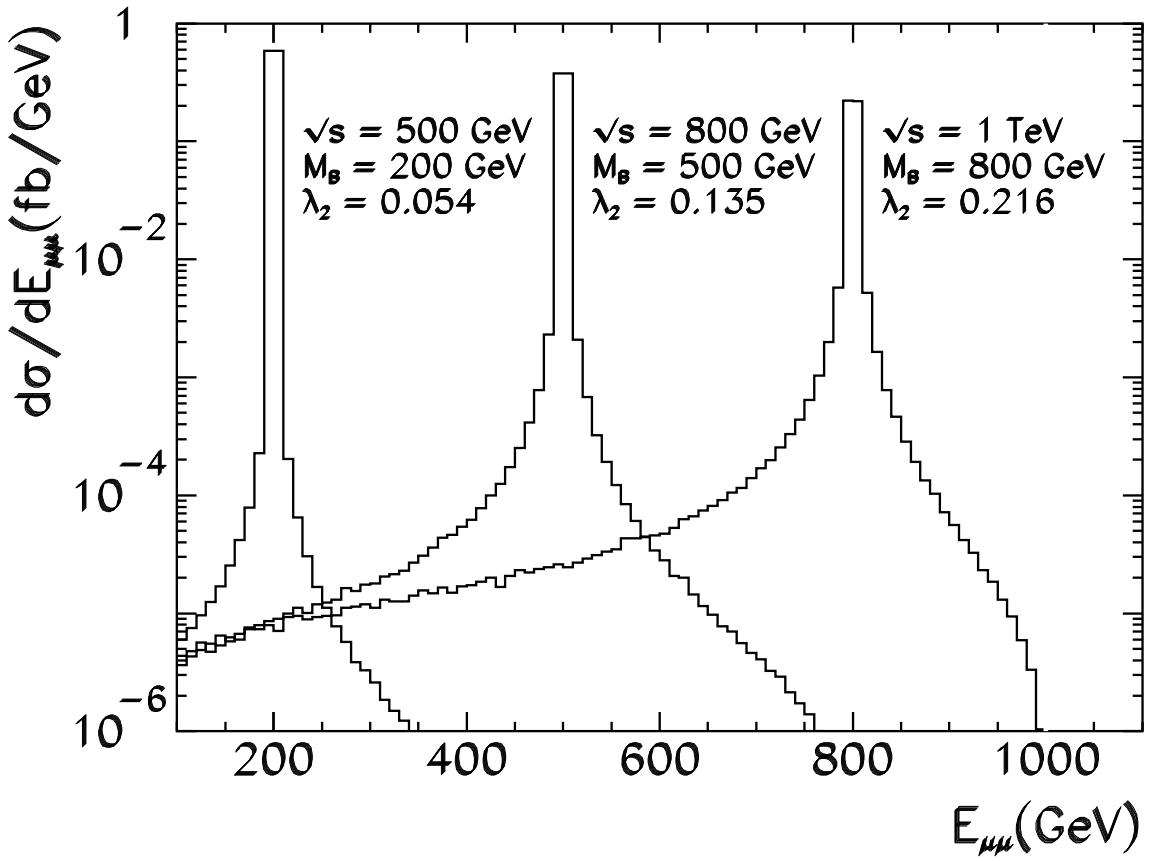

FIG. 4. Cross-sections for the $\mu^{\pm}\mu^{\pm}$ production in $e^{+}e^{-}$ colliders as a function of their total invariant mass $E_{\mu\mu}$.

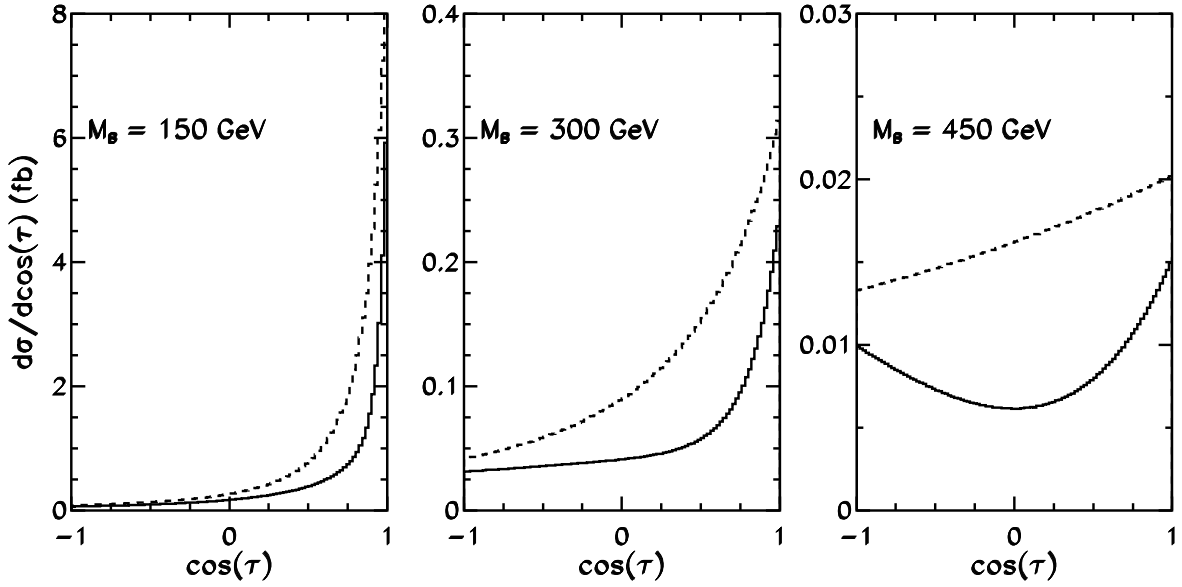

FIG. 5. Angular distribution in laboratory frame at $\sqrt{s} = 500$ GeV. The solid (dashed) line corresponds to vector (scalar) bileptons.

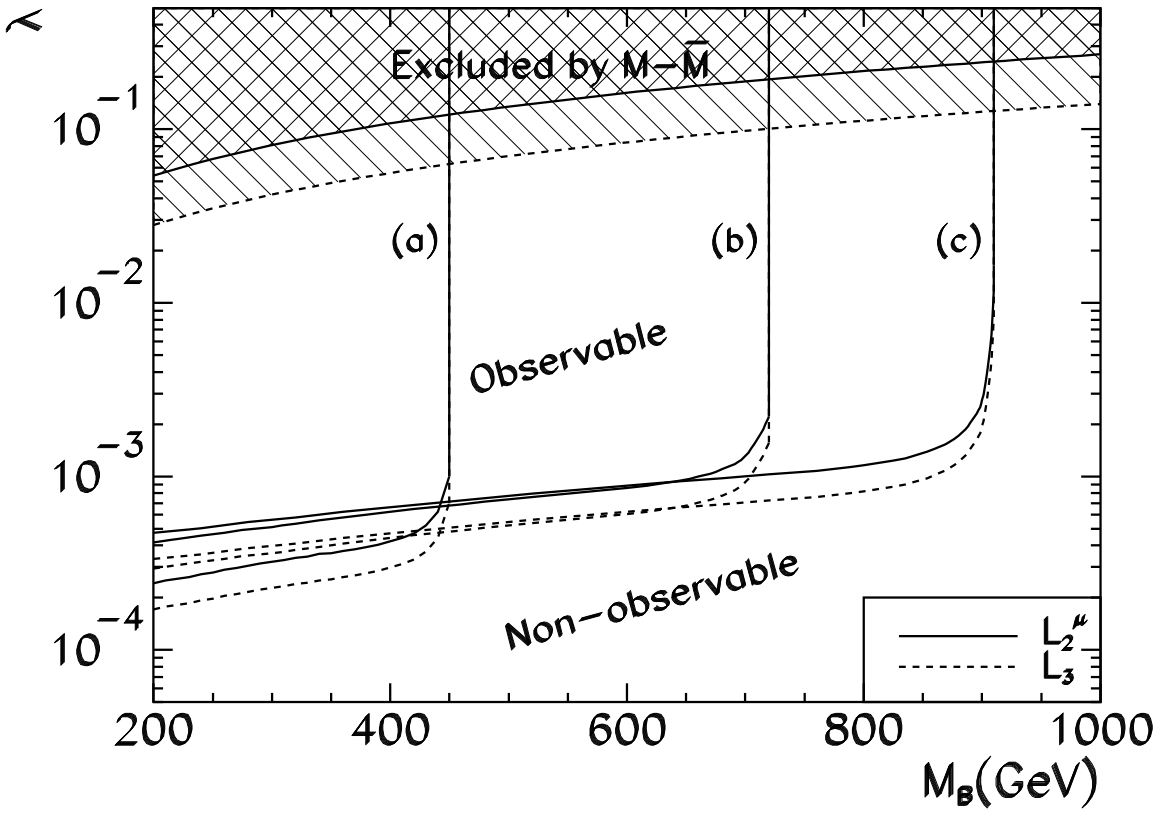

FIG. 6. The same as Fig. 3 for the $e\gamma$ mode of the linear collider.

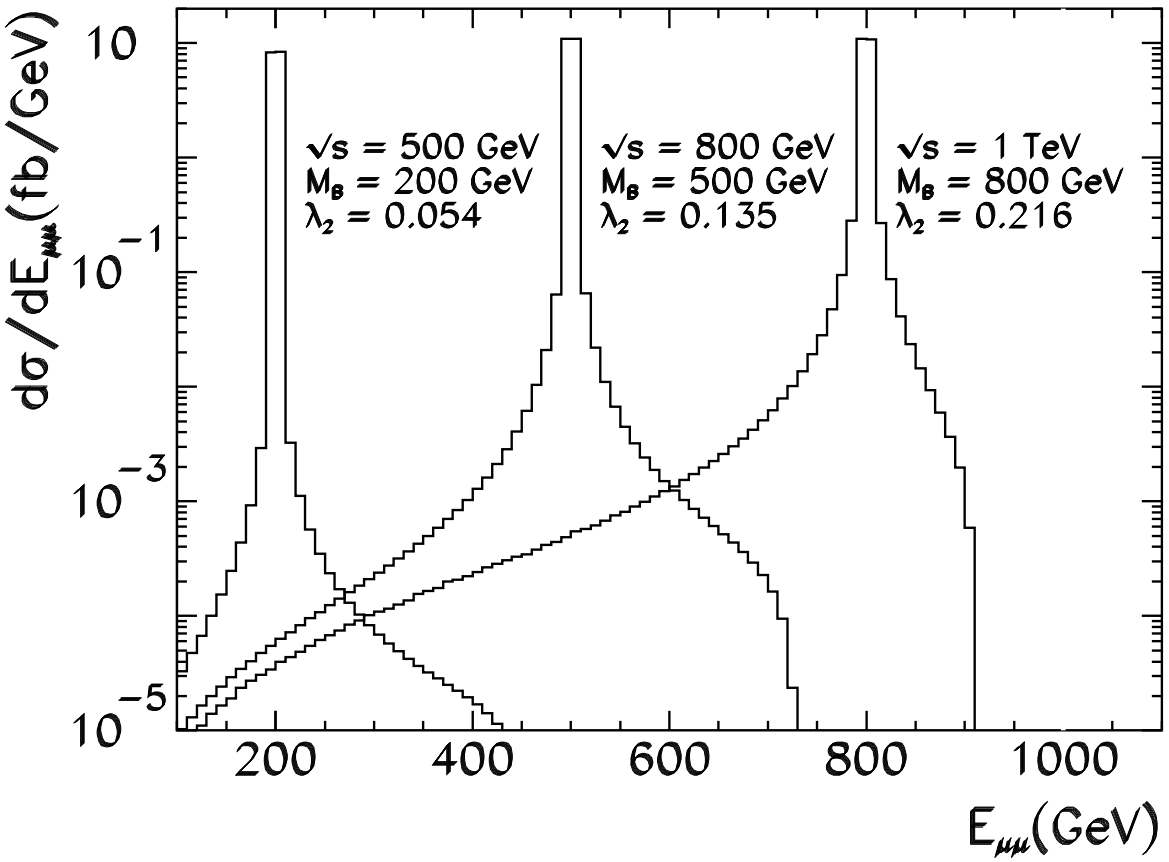

FIG. 7. Cross sections for the $\mu^{\pm}\mu^{\pm}$ production in $e\gamma$ colliders as a function of their total invariant mass $E_{\mu\mu}$.